

## Structures of Lanthanide Complexes of $\beta$ -Ketophosphoryl Compounds†

Ryszard Babecki,<sup>a</sup> Andrew W. G. Platt<sup>\*,a</sup> and John Fawcett<sup>b</sup>

<sup>a</sup> Chemistry Division, Department of Applied Science, Staffordshire Polytechnic, College Road, Stoke on Trent ST4 2DE, UK

<sup>b</sup> Department of Chemistry, The University, Leicester LE1 7RH, UK

Complexes of lanthanide nitrates and perchlorates with the  $\beta$ -ketophosphoryl ligands  $\text{Ph}_2\text{P}(\text{O})\text{CH}_2\text{C}(\text{O})\text{Ph}$  (pdppo) and  $(\text{BuO})_2\text{P}(\text{O})\text{CH}_2\text{C}(\text{O})\text{Ph}$  (dbpp) have been synthesised and studied by X-ray crystallography, and infrared and NMR spectroscopies. The structures of the lanthanide nitrate complexes with pdppo were found to change in the solid state between the lighter and heavier lanthanides, but form an isostructural series in solution. The X-ray structure of  $[\text{Er}(\text{NO}_3)_3(\text{pdppo})_2(\text{OH}_2)]$  ( $R' = 0.031$  for 6898 diffractometer observed reflections) shows the metal to be nine-co-ordinated in a distorted tricapped trigonal prism. Both H atoms of the co-ordinated water molecule are involved in hydrogen bonding, one to the carbonyl oxygen of the ligand, and the other to an oxygen atom of a nitrate group of an adjacent molecule. Perchlorate complexes of pdppo have the same composition for the solid complexes but show small structural changes in solution. The complexes of dbpp are all oils. The nitrates appear to be twelve-co-ordinate and isostructural in solution. The perchlorate complexes of dbpp appear to exist as two distinct isostructural classes in solution.

The co-ordination chemistry of lanthanides continues to attract interest both as a field of study in its own right<sup>1-3</sup> and for its application to synthetic organic chemistry.<sup>4,5</sup> The use of difunctional ligands has also received some attention, due in part to the variety of co-ordination modes possible<sup>6-8</sup> and their potential application to solvent extraction.<sup>9,10</sup>

Structural information on lanthanide complexes comes, for the most part, from determination of the solid-state structures by X-ray diffraction. The elucidation of structures in solution poses an interesting problem due to the paramagnetism of most of the lanthanide ions, and much effort has been expended on the analysis of lanthanide-induced NMR shifts as a probe for solution structures.<sup>11,12</sup> It is obviously of interest to compare the results of such solution studies with structural information obtained on the isolated complexes. In this paper we present the results of such a study for a series of lanthanide nitrate and perchlorate complexes of phenacyldiphenylphosphine oxide,  $\text{Ph}_2\text{P}(\text{O})\text{CH}_2\text{C}(\text{O})\text{Ph}$  (pdppo) and dibutyl phenacylphosphonate,  $(\text{BuO})_2\text{P}(\text{O})\text{CH}_2\text{C}(\text{O})\text{Ph}$  (dbpp).

### Results and Discussion

**Nitrate Complexes of pdppo.**—All complexes were obtained as crystalline solids which melt without decomposition. They are poorly soluble in most organic solvents but dissolve in nitromethane, in which they are non-conducting. Full characterising data are given in Table 1.

Two structural classes of complex are formed,  $[\text{Ln}(\text{NO}_3)_3(\text{pdppo})_3]$  for the lighter lanthanides ( $\text{Ln} = \text{La}$  and  $\text{Ce}$ ) and  $[\text{Ln}(\text{NO}_3)_3(\text{pdppo})_2(\text{OH}_2)]$  for the heavier metals ( $\text{Ln} = \text{Pr-Lu}$ ). To characterise fully the structural changes occurring in the solid state, representative complexes from the two structural divisions were examined by single-crystal X-ray diffraction. The structure of  $[\text{Ce}(\text{NO}_3)_3(\text{pdppo})_3]$  **2** has recently been published elsewhere<sup>13</sup> and shows (Fig. 1) that two ligands are monodentate, bonding through the phosphoryl oxygen

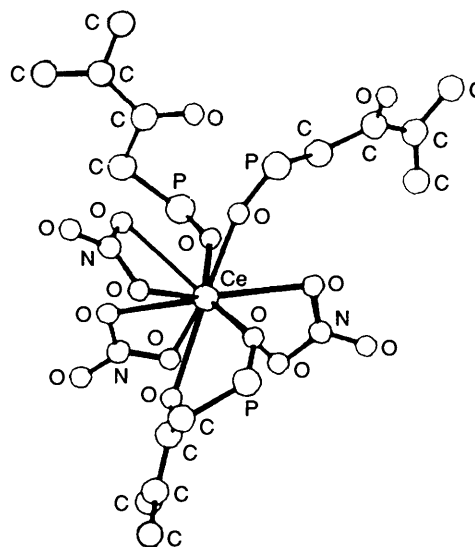


Fig. 1 The structure of  $[\text{Ce}(\text{NO}_3)_3(\text{pdppo})_3]$  (phenyl groups omitted for clarity)

atom only, whilst the third chelates *via* phosphoryl and carbonyl oxygens.

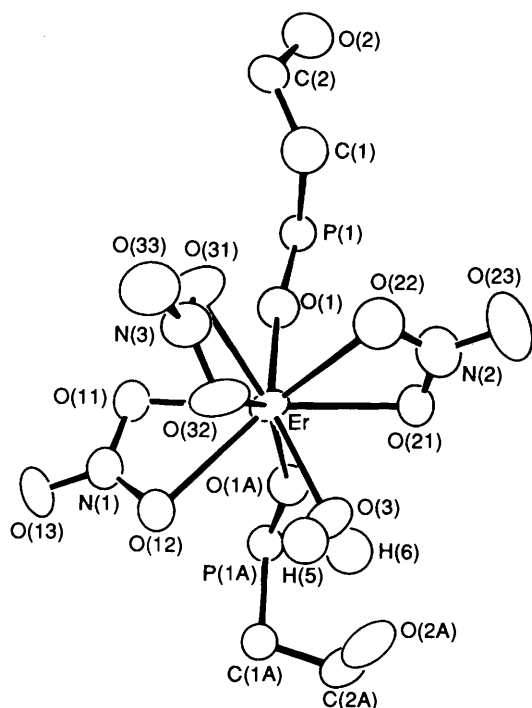
The complex  $[\text{Er}(\text{NO}_3)_3(\text{pdppo})_2(\text{OH}_2)]$  **10** crystallises with two discrete molecules in the unit cell having the structure shown in Fig. 2. Selected bond lengths and angles are given in Table 2, and the atomic coordinates in Table 3. The geometry about the erbium atom is complex and does not conform to any simple idealised polyhedron, but can be considered as a distorted tricapped trigonal prism with the oxygen atoms of the pdppo ligands and the water molecule capping a trigonal prism defined by the nitrate oxygens. Alternatively, if nitrate ions are considered as occupying single co-ordination sites, then the geometry approximates to a distorted octahedron, with the nitrate groups occupying the meridional positions. Neither of the carbonyl oxygens is directly bonded to the metal. Both hydrogen atoms of the co-ordinated water molecule were

† Supplementary data available: see Instructions for Authors, *J. Chem. Soc., Dalton Trans.*, 1992, Issue 1, pp. xx-xxv.

**Table 1** Characterising data for  $[\text{Ln}(\text{NO}_3)_3(\text{pdppo})_x(\text{OH}_2)_y]$ 

Complex			Analysis (%) <sup>a</sup>			Infrared ( $\text{cm}^{-1}$ ) <sup>b</sup>			
Ln	x	y	C	H	N	$\nu(\text{CO})$	$\nu(\text{PO})$	$^{31}\text{P}$ NMR( $\delta$ ) <sup>c</sup>	M.p./ $^{\circ}\text{C}$
1 La	3	0	53.90 (56.05)	3.95 (4.00)	3.55 (3.25)	1630	1160 1150	32.5	199.0
2 Ce	3	0	55.85 (56.00)	4.00 (4.00)	3.25 (3.25)	1655 1670	1160 1150	45.5	97.0
3 Pr	2	1	49.00 (48.75)	3.50 (3.70)	4.20 (4.25)	1655 1675	1150 1165	64.0	146.5
4 Nd	2	1	48.80 (48.60)	3.70 (3.65)	4.05 (4.25)	1660	1155 1170	59.2	129.6
5 Sm	2	1	48.40 (48.30)	3.60 (3.65)	4.05 (4.20)	1660	1155 1170	29.9	151.5
6 Eu	2	1				1660	1150 1170	-29.2	151.5
7 Gd	2	1	47.95 (47.95)	3.55 (3.60)	4.10 (4.20)	1660	1150 1170	Not observed	159.5
8 Dy	2	1	48.25 (47.70)	3.60 (3.60)	4.10 (4.20)	1660	1150 1170	-19.5	161.1
9 Ho	2	1	47.70 (47.60)	3.40 (3.50)	4.15 (4.15)	1660	1155 1170	26.9	165.0
10 Er	2	1	47.35 (47.50)	3.45 (3.60)	4.20 (4.15)	1660	1165 1175	-75.0	165.6
11 Yb	2	1	47.80 (47.20)	3.70 (3.55)	4.05 (4.15)	1660	1160 1175	28.0	171.7
12 Lu	2	1	47.10 (47.10)	3.45 (3.45)	4.00 (4.10)	1660	1160 1180	35.6	166.7

<sup>a</sup> Calculated values in parentheses. <sup>b</sup> As KBr discs. Spectra run as Nujol mulls showed identical features with bands assigned to co-ordinated water present. <sup>c</sup> In nitromethane solution.

**Fig. 2** The structure of  $[\text{Er}(\text{NO}_3)_3(\text{pdppo})_2(\text{OH}_2)]$  (phenyl groups omitted for clarity)

located and found to be involved in hydrogen-bonding interactions: H(6) is hydrogen bonded to a carbonyl oxygen in the same molecule giving an eight-membered ring similar to that found in  $[\text{Er}(\text{NO}_3)_3\{\text{Pr}^{\text{I}}\text{O}\}_2\text{P}(\text{O})\text{CH}_2\text{C}(\text{O})\text{NEt}_2\}(\text{OH}_2)]$ ,<sup>14</sup> H(5) is involved in intermolecular hydrogen bonding to O(12) of a nitrate group in an adjacent molecule. Although the hydrogen bonding of H(6) to O(2A) does not cause a significant lengthening of the C=O bond, its effect can be seen in the lessening of the dihedral angle between the plane of the phenyl ring and that of the carbonyl group. This

**Table 2** Selected bond lengths ( $\text{\AA}$ ) and angles ( $^{\circ}$ ) for  $[\text{Er}(\text{NO}_3)_3(\text{pdppo})_2(\text{OH}_2)]$ 

Er-O(1)	2.253(3)	O(1)-P(1)	1.497(3)
Er-O(1A)	2.247(3)	O(1A)-P(1A)	1.479(4)
Er-O(11)	2.432(3)	P(1)-C(1)	1.812(5)
Er-O(12)	2.472(3)	P(1A)-C(1A)	1.822(4)
Er-O(21)	2.432(3)	C(1)-C(2)	1.518(6)
Er-O(22)	2.410(5)	C(1A)-C(2A)	1.511(6)
Er-O(31)	2.444(3)	C(2)-O(2)	1.219(5)
Er-O(32)	2.422(3)	C(2A)-O(2A)	1.210(7)
Er-O(3)	2.323(3)	O(2A)-H(6)	1.970
		O(3)-H(6)	0.782(3)
		O(3)-H(5)	0.837(3)
		O(12)-H(5)	1.975
O(1)-Er-O(1A)	83.7(1)	O(1)-Er-O(3)	152.0(1)
O(1A)-Er-O(3)	83.9(1)	O(1)-Er-N(1)	78.5
O(1)-Er-N(2)	100.0	O(1)-Er-N(3)	96.9
O(1A)-Er-N(1)	99.3	O(1A)-Er-N(2)	160.4
O(1A)-Er-N(3)	77.1	O(3)-Er-N(1)	78.8
O(3)-Er-N(2)	103.1	O(3)-Er-N(3)	76.7
N(1)-Er-N(2)	100.0	N(1)-Er-N(3)	176.3
N(2)-Er-N(3)	83.5	O(3)-H(6)-O(2A)	162.8
C(1A)-C(2A)-O(2A)	111.3(2)	C(1)-C(2)-O(2)	118.8(3)

angle is  $6.1^{\circ}$  for the hydrogen-bonded ligand compared with  $16.5^{\circ}$  for the carbonyl group not involved in any secondary interaction. A similar effect is seen in the cerium complex  $[\text{Ce}(\text{NO}_3)_3(\text{pdppo})_3]$ .<sup>13</sup> These changes in dihedral angle are consistent with the expected increase in conjugation between the phenyl ring and carbonyl group when the ligand is involved in co-ordination or hydrogen bonding through the carbonyl oxygen.

In both complexes the nitrate groups act as bidentate ligands. The Er-O( $\text{NO}_3$ ) distances compare well with those found in the related complex  $[\text{Er}(\text{NO}_3)_3\{\text{Pr}^{\text{I}}\text{O}\}_2\text{P}(\text{O})\text{CH}[\text{C}(\text{O})\text{NEt}_2]\text{CH}_2\text{C}(\text{O})\text{NEt}_2\}(\text{OH}_2)]$ .<sup>15</sup> In this complex the Er-O distances vary from 2.473 to 2.403  $\text{\AA}$  with an average of 2.431  $\text{\AA}$ . A similar variation of bond length is seen in complex 10 where the

**Table 3** Fractional atomic coordinates for [Er(NO<sub>3</sub>)<sub>3</sub>(pdppo)<sub>2</sub>(OH<sub>2</sub>)]

Atom	x	y	z	Atom	x	y	z
Er	0.013 81(2)	0.321 66(1)	0.433 23(1)	C(12A)	0.002 68(23)	0.256 33(13)	-0.121 92(19)
P(1)	0.110 84(9)	0.127 89(5)	0.389 32(9)	C(13A)	-0.072 99(23)	0.208 79(13)	-0.254 20(19)
O(1)	0.088 54(26)	0.207 88(14)	0.394 66(27)	C(14A)	-0.193 76(23)	0.169 06(13)	-0.288 49(19)
O(2)	0.178 1(3)	-0.003 48(17)	0.541 3(3)	C(15A)	-0.238 89(23)	0.176 88(13)	-0.190 54(19)
C(1)	0.097 7(4)	0.112 36(23)	0.529 6(4)	C(16A)	-0.163 25(23)	0.224 44(13)	-0.058 26(19)
C(2)	0.195 8(4)	0.065 84(23)	0.596 3(4)	H(12A)	0.096 19(23)	0.028 71(13)	-0.095 73(19)
C(11)	-0.005 10(22)	0.059 58(11)	0.240 19(19)	H(13A)	-0.038 06(23)	0.202 73(13)	-0.330 05(19)
C(12)	-0.069 58(22)	0.084 98(11)	0.133 32(19)	H(14A)	-0.252 35(23)	0.132 24(13)	-0.390 90(19)
C(13)	-0.160 22(22)	0.033 91(11)	0.010 28(19)	H(15A)	-0.332 42(23)	0.146 13(13)	-0.217 10(19)
C(14)	-0.186 40(22)	-0.042 56(11)	-0.005 92(19)	H(16A)	-0.198 18(23)	0.230 51(13)	0.017 58(19)
C(15)	-0.121 94(22)	-0.067 95(11)	0.100 93(19)	C(21A)	0.210 31(21)	0.338 89(16)	0.177 6(3)
C(16)	-0.031 29(22)	-0.016 88(11)	0.223 99(19)	C(22A)	0.271 19(21)	0.277 40(16)	0.206 0(3)
H(12)	-0.049 31(22)	-0.144 19(11)	0.145 87(19)	C(23A)	0.404 49(21)	0.277 30(16)	0.237 4(3)
H(13)	-0.210 13(22)	0.053 57(11)	-0.072 45(19)	C(24A)	0.476 89(21)	0.338 68(16)	0.240 4(3)
H(14)	-0.256 58(22)	-0.082 11(11)	-0.101 19(19)	C(25A)	0.416 01(21)	0.400 15(16)	0.212 0(3)
H(15)	-0.142 19(22)	-0.127 17(11)	-0.088 40(19)	C(26A)	0.282 72(21)	0.400 26(16)	0.180 6(3)
H(16)	0.018 64(22)	-0.036 54(11)	0.306 72(19)	H(22A)	0.215 14(21)	0.229 90(16)	0.203 7(3)
C(21)	0.270 46(18)	0.112 65(13)	0.398 64(27)	H(23A)	0.451 62(21)	0.229 71(16)	0.259 4(3)
C(22)	0.364 79(18)	0.176 39(13)	0.449 84(27)	H(24A)	0.580 09(21)	0.338 60(16)	0.264 7(3)
C(23)	0.489 70(18)	0.166 68(13)	0.455 78(27)	H(25A)	0.472 07(21)	0.447 67(16)	0.214 3(3)
C(24)	0.520 31(18)	0.093 24(13)	0.410 52(27)	H(26A)	0.235 58(21)	0.447 85(16)	0.158 6(3)
C(25)	0.425 99(18)	0.029 51(13)	0.359 31(27)	C(31A)	-0.241 30(25)	0.407 31(17)	-0.069 64(22)
C(26)	0.301 07(18)	0.039 19(13)	0.353 39(27)	C(32A)	-0.187 08(25)	0.400 45(17)	-0.160 46(22)
H(22)	0.341 08(18)	0.233 27(13)	0.484 88(27)	C(33A)	-0.268 48(25)	0.388 49(17)	-0.294 57(22)
H(23)	0.562 72(18)	0.216 04(13)	0.495 43(27)	C(34A)	-0.404 12(25)	0.383 42(17)	-0.337 87(22)
H(24)	0.617 03(18)	0.085 72(13)	0.415 11(27)	C(35A)	-0.458 33(25)	0.390 29(17)	-0.247 07(22)
H(25)	0.449 70(18)	-0.027 36(13)	0.324 29(27)	C(36A)	-0.376 92(25)	0.402 23(17)	-0.112 95(22)
H(26)	0.228 05(18)	-0.010 14(13)	0.313 74(27)	H(32A)	-0.082 09(25)	0.404 37(17)	-0.126 92(22)
C(31)	0.304 57(26)	0.104 67(18)	0.724 27(24)	H(33A)	-0.226 51(25)	0.383 18(17)	-0.364 86(22)
C(32)	0.372 04(26)	0.060 03(18)	0.798 61(24)	H(34A)	-0.467 15(25)	0.374 17(17)	-0.441 70(22)
C(33)	0.478 94(26)	0.094 25(18)	0.922 60(24)	H(35A)	-0.563 33(25)	0.386 35(17)	-0.280 59(22)
C(34)	0.518 36(26)	0.173 09(18)	0.972 26(24)	H(36A)	-0.418 89(25)	0.407 54(17)	-0.042 65(22)
C(35)	0.450 87(26)	0.217 73(18)	0.897 93(24)	O(3)	-0.148 32(26)	0.398 87(15)	0.382 60(27)
C(36)	0.343 99(26)	0.183 53(18)	0.773 94(24)	N(1)	0.241 3(3)	0.425 32(19)	0.502 2(3)
H(32)	0.341 52(26)	-0.001 01(18)	0.760 15(24)	O(11)	0.245 28(28)	0.356 71(17)	0.498 1(3)
H(33)	0.531 19(26)	0.059 70(18)	0.980 15(24)	O(12)	0.127 63(28)	0.445 78(16)	0.472 3(3)
H(34)	0.601 13(26)	0.199 59(18)	1.068 25(24)	O(13)	0.336 2(3)	0.467 22(21)	0.529 4(5)
H(35)	0.481 40(26)	0.278 78(18)	0.936 39(24)	N(2)	-0.215 4(4)	0.219 95(24)	0.348 2(4)
H(36)	0.039 41(9)	0.218 07(18)	0.716 39(24)	O(21)	-0.187 12(26)	0.236 48(16)	0.266 05(27)
P(1A)	0.004 81(26)	0.332 50(5)	0.137 31(9)	O(22)	-0.138 3(3)	0.251 72(22)	0.469 4(3)
O(1A)	-0.217 8(3)	0.310 25(15)	0.231 81(24)	O(23)	-0.310 7(4)	0.174 6(3)	0.312 0(5)
O(2A)	-0.015 6(4)	0.415 02(21)	0.140 3(3)	N(3)	0.094 0(4)	0.377 03(20)	0.716 0(3)
C(1A)	-0.163 3(4)	0.423 01(21)	0.125 7(4)	O(31)	0.132 7(3)	0.318 14(19)	0.659 1(3)
C(2A)	-0.042 45(23)	0.415 74(23)	0.070 0(4)	O(32)	0.018 7(4)	0.409 07(17)	0.641 29(29)
C(11A)	-0.042 45(23)	0.264 17(13)	-0.023 96(19)	O(33)	0.126 0(4)	0.401 74(20)	0.835 1(3)

range of Er–O distances is 2.472–2.410 Å with an average of 2.435 Å. Interestingly, in the nine-co-ordinate complex [Er(NO<sub>3</sub>)<sub>3</sub>{Pr<sup>II</sup>P(O)CH[C(O)NEt<sub>2</sub>][CH<sub>2</sub>C(O)NEt<sub>2</sub>}]<sup>16</sup> the Er–O(NO<sub>3</sub>) bond lengths are much more regular with a shorter average distance of 2.407 Å. Thus it seems possible that the variations in Er–O distances are due to steric crowding.

The Er–O(H<sub>2</sub>O) distance is virtually identical with the value reported for the related compound above<sup>15</sup> and at 2.323 Å intermediate between values found in [Er(NO<sub>3</sub>)<sub>3</sub>{(Pr<sup>II</sup>O)<sub>2</sub>P(O)CH<sub>2</sub>C(O)NEt<sub>2</sub>}(OH<sub>2</sub>)] (2.302 Å),<sup>14</sup> [Er(OH<sub>2</sub>)<sub>2</sub>LCl<sub>2</sub>]Cl<sup>17</sup> (2.311 Å) and longer distances in [Er(OH<sub>2</sub>)<sub>2</sub>LCl<sub>3</sub>]·2H<sub>2</sub>O (L = 12-crown-4 = 1,4,7,10-tetraoxacyclododecane) where the values range from 2.310 to 2.481 Å.<sup>17</sup>

Preliminary work on the unit-cell dimensions of the dysprosium complex **8** showed it to be isostructural with **10**, and its structure was not further investigated.

**Infrared spectra.** The differing modes of co-ordination of pdppo identified crystallographically can be seen in the infrared spectra of complexes **2** and **10**. Thus two CO stretches are seen for **2**. Similarly, two CO absorptions are seen for the praseodymium complex **3**, the lower-frequency band being assigned to the hydrogen-bonded CO group. For complexes **4–12** a single broad CO absorption is seen in the spectra run as KBr discs and

as Nujol mulls. This is presumably due to the presence of two closely spaced, and hence unresolved, bands.

Crystallographically confirmed bidentate nitrate groups give strong absorptions between 1480–1435 and 1310–1300 cm<sup>-1</sup> for [Ln(NO<sub>3</sub>)<sub>3</sub>(dmsO)<sub>n</sub>] complexes (n = 3 or 4, dmsO = dimethyl sulfoxide)<sup>18</sup> and between 1480–1460 and 1310–1285 cm<sup>-1</sup> for lanthanide nitrate complexes of 2,7-dimethyl-1,8-naphthyridine.<sup>19</sup> These values compare with ranges of 1500–1450 and 1305–1285 cm<sup>-1</sup> for the pdppo complexes. Bidentate co-ordination is confirmed for the complexes of Ce and Er and thus almost certainly occurs throughout the series. The co-ordinated water molecule shows two OH stretches at about 3350 and 3250 cm<sup>-1</sup>. The frequencies are consistent with the observed hydrogen bonding.<sup>20</sup>

<sup>31</sup>P NMR spectra. Although NMR spectroscopy of paramagnetic molecules does not, in general, yield detailed structural information, analysis of the lanthanide-induced shifts for a series of related complexes has been shown to give indications of changes in structure across the series of lanthanide complexes.<sup>11,12</sup> The lanthanide-induced shifts are analysed by plotting  $\delta_i / \langle S_z \rangle_i$  vs.  $D_i / \langle S_z \rangle_i$  and  $\delta_i / D_i$  vs.  $\langle S_z \rangle_i / D_i$  where  $\langle S_z \rangle_i$  is the spin expectation value and  $D_i$  is related to the variation in paramagnetic shift which should

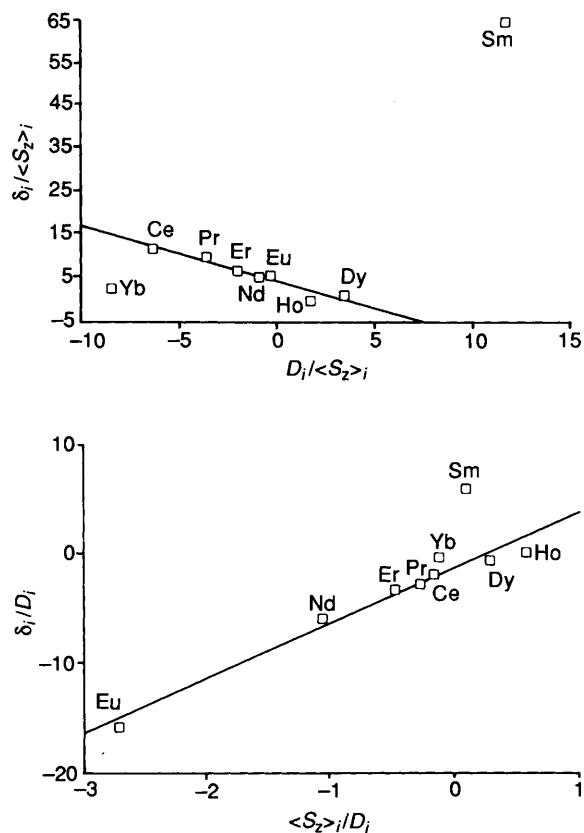


Fig. 3 Plots of the lanthanide-induced shifts for lanthanide nitrate complexes with pdppo

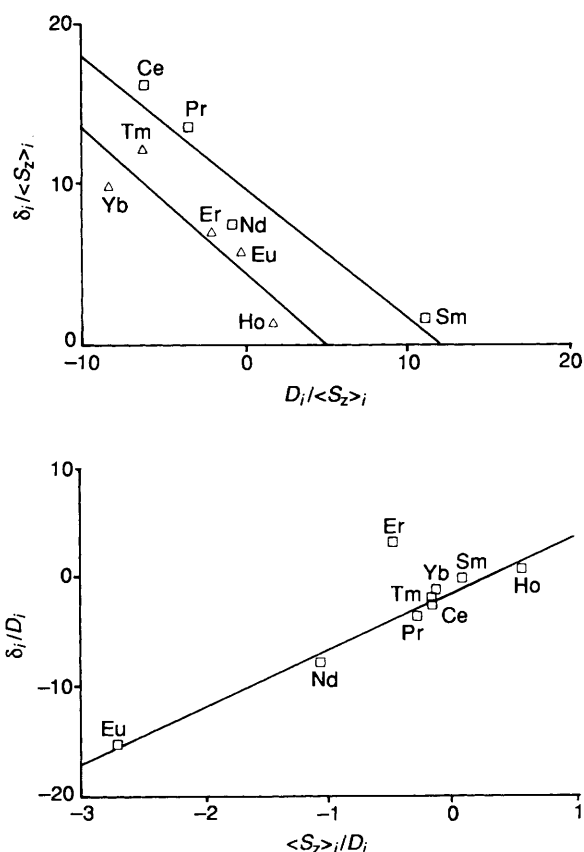


Fig. 4 Plots of the lanthanide-induced shifts for lanthanide perchlorate complexes of pdppo

occur if the crystal-field coefficients are independent of the lanthanide ion;  $\langle S_z \rangle_i$  and  $D_i$  are characteristics of a particular lanthanide ion and their values have been calculated.<sup>21,22</sup>

The paramagnetic shift  $\delta_i$  is given by  $\delta_{Ln} - \frac{1}{2}(\delta_{La} + \delta_{Lu})$ , where  $\delta_{Ln}$  is the observed shift for a given lanthanide and  $\delta_{La}$  and  $\delta_{Lu}$  are the shifts of the diamagnetic lanthanum and lutetium complexes. If the complexes are essentially isostructural across the series, then both plots are expected to be linear, whilst if a major structural change occurs, for example change of co-ordination number or from mono- to bi-dentate co-ordination of a ligand, then both plots are expected to show a break. Minor changes in structure are implied if the plot of  $\delta_i / \langle S_z \rangle_i$  vs.  $D_i / \langle S_z \rangle_i$  shows a break whilst  $\delta_i / D_i$  vs.  $\langle S_z \rangle_i / D_i$  remains linear.

The results of the lanthanide-induced shifts in nitromethane are shown in Fig. 3. In both cases good linear plots are obtained (regression coefficients of 0.90 and 0.98 respectively) if the points for Sm and Yb are disregarded. There is no obvious reason for the anomalous values for Sm and Yb, but similar effects have been observed previously.<sup>11,12</sup> This implies that in nitromethane solution the compounds form an isostructural series, in contrast to the differences observed in the solid state. For high co-ordination numbers there is likely to be little energy difference between alternative structures. Thus solid-state effects brought about by the small changes in ionic radii are probably responsible for the changes in co-ordination geometry observed. The fact that complexes with differing stoichiometries appear isostructural in solution could be due to rapid dissociation of the third pdppo ligand from complexes 1 and 2, an average shift thus being observed. This has been confirmed by the observation of a single resonance in the <sup>31</sup>P NMR spectrum on addition of free pdppo to solutions of the complexes. The use of this average shift in the subsequent analysis is unlikely to cause significant error since the observed shifts are close to those of the free ligand itself.

**Perchlorate Complexes of pdppo.**—The complexes were obtained as microcrystalline powders which are only sparingly soluble in common organic solvents. The solubilities decrease markedly with increasing atomic weight of the lanthanide. The characterising data are given in Table 4. In the solid state the complexes all have a composition  $\text{Ln}(\text{ClO}_4)_3(\text{pdppo})_4(\text{OH}_2)$ , and are stable at room temperature, but most decompose violently on melting at about 300 °C. Owing to the poor solubility of the compounds it has not been possible to grow single crystals suitable for X-ray diffraction work, and thus detailed knowledge of the co-ordination geometries cannot be obtained.

**Infrared spectra.** In principle the same type of information that was deduced for the nitrate complexes should be obtainable for the perchlorates. The absorptions due to the CO groups occur as a broad band between 1670 and 1650  $\text{cm}^{-1}$  (often with ill defined absorption maxima), together with a sharp, more intense, band at around 1630  $\text{cm}^{-1}$ . This indicates that a mixture of bonding modes of the pdppo ligand is occurring, presumably monodentate, hydrogen-bonding and/or chelating all being present.

The state of co-ordination of the perchlorate ion is more difficult to ascertain. The distinction between ionic, mono- and bi-dentate perchlorate by infrared spectroscopy is well established.<sup>20</sup> However, for the present complexes the absorption bands from perchlorate overlap with those of the co-ordinated P=O group. It is apparent from the number of absorptions not attributable to the ligand that, in addition to ionic  $\text{ClO}_4^-$  which gives rise to a broad, intense absorption at about 1085  $\text{cm}^{-1}$ , co-ordinated perchlorate groups are also present.

**<sup>31</sup>P NMR spectra.** Although the complexes are insoluble in many organic solvents they are sufficiently soluble in nitromethane to permit measurement of the phosphorus NMR spectra. The lanthanide-induced shifts were analysed as before and the results are shown in Fig. 4. A good linear plot ( $R^2 = 0.98$ ) is obtained for  $\delta_i / D_i$  vs.  $\langle S_z \rangle_i / D_i$  whilst the plot of

**Table 4** Characterising data for  $[\text{Ln}(\text{ClO}_4)_3(\text{pdppo})_4(\text{OH}_2)]$ 

Complex	Analysis (%) <sup>a</sup>		<sup>31</sup> P NMR ( $\delta$ ) <sup>b</sup>	Infrared <sup>c</sup> $\nu(\text{CO})/\text{cm}^{-1}$	$\Lambda^d/\Omega^{-1} \text{ cm}^2 \text{ mol}^{-1}$	M.p./°C
	Ln	C				
13 La	56.00 (55.90)	4.05 (3.70)	36.5	1660		308 (decomp.)
14 Ce	55.70 (55.30)	3.95 (4.05)	54.1	1660, 1632, 1625		249
15 Pr	55.20 (55.25)	4.15 (4.05)	78.6	1670, 1625		268
16 Nd	55.75 (55.15)	3.95 (4.05)	71.7	1670, 1660, 1625	213	280
17 Sm	55.35 (54.95)	3.95 (4.05)	38.5	1665, 1650, 1625	185	288 (decomp.)
18 Eu	55.70 (54.90)	3.90 (4.05)	-22.8	1670, 1650, 1625		302 (decomp.)
19 Gd	55.05 (54.75)	4.10 (3.95)	10.9	1670, 1655		307 (decomp.)
20 Ho			9.9	1660, 1630		308 (decomp.)
21 Er	52.25 (54.45)	4.00 (4.00)	-69.1	1665, 1630	195	309 (decomp.)
22 Tm	55.00 (54.40)	3.80 (4.00)	-61.1	1665, 1655, 1630		306 (decomp.)
23 Yb	54.80 (54.25)	3.80 (4.00)	13.1	1660, 1635	181	306 (decomp.)
24 Lu	54.35 (54.20)	3.80 (4.00)	40.4	1660, 1635		306 (decomp.)

<sup>a</sup> Calculated values in parentheses. <sup>b</sup> In nitromethane. <sup>c</sup> As Nujol mulls; all complexes gave a broad absorption at  $3400 \text{ cm}^{-1}$  due to water and two peaks at  $1150$  and  $1140 \text{ cm}^{-1}$  assigned as P=O stretches. <sup>d</sup> For  $10^{-3} \text{ mol dm}^{-3}$  solutions in nitromethane.

**Table 5** Characterising data for complexes of dbpp $[\text{Ln}(\text{NO}_3)_3(\text{dbpp})_4(\text{OH}_2)_2]$ 

Complex	Ln	<sup>31</sup> P NMR ( $\delta$ ) <sup>a</sup>
25	La	19.9
26	Ce	32.0
27	Pr	68.6
28	Nd	85.6
29	Eu	-65.9
30	Dy	-142.8
31	Er	
32	Tm	-115.5
33	Lu	21.1

 $[\text{Ln}(\text{ClO}_4)_3(\text{dbpp})_x(\text{OH}_2)_2]$ 

Ln	x	<sup>31</sup> P NMR ( $\delta$ )	Infrared ( $\text{cm}^{-1}$ ) <sup>b</sup>	
			$\nu(\text{CO})$	$\nu(\text{PO})$
34 La	4	20.6	1630	1190
35 Ce	4	52.8	1660	1200
36 Pr	4	100.6	1675, 1640	1185, 1200
37 Nd	4	105.0	1640	1190
38 Sm	4	21.2	1650, 1640	1195
39 Eu	3	-108.0	1675, 1640	1195
40 Er	3	-154.2	1660	1190
41 Tm	3	-103.2	1670	1200
42 Yb	3	-5.9	1670, 1650	1195
43 Lu	3	21.4	1675, 1640	1195

Infrared data complexes 25–33:  $\nu(\text{CO})$  1675;  $\nu(\text{PO})$  1220, 1180  $\text{cm}^{-1}$ . Elemental analysis [Found (Calc.)]: complex, 27, C, 47.05 (47.70); H, 6.50 (6.50); N, 2.90 (2.60); 31, C, 45.40 (46.90); H, 6.40 (6.40); N, 2.80 (2.55); 36, C, 44.50 (44.55); H, 6.20 (6.10); 40, C, 40.65 (40.10); H, 5.95 (5.55)%.

<sup>a</sup> In nitromethane. <sup>b</sup> As contact films.

$\delta_i / \langle S_z \rangle_i$  vs.  $D_i / \langle S_z \rangle_i$  shows a clear distinction between the lighter lanthanides (La–Sm) and the heavier ones (Eu–Lu). These results indicate that only minor structural changes are occurring across the series.

This is broadly in accord with the available solid-state data where the composition and spectroscopic properties were uniform throughout. Although the majority of complexes were not soluble enough to permit conductivity measurements, in a few cases the values could be measured. These values fall within the accepted range for 2:1 electrolytes in nitromethane,<sup>23</sup> confirming that one perchlorate remains bonded to the metal in solution. However, in many cases, prolonged reflux was required to bring about solution, and it is possible that the dissolution process was accompanied by a structural change. Direct comparison of the solution and solid-state structures by infrared spectroscopy is not possible, as nitromethane has

intense absorptions in the carbonyl and perchlorate regions of the spectrum. Although most of the complexes are insoluble in  $\text{CDCl}_3$ , the lanthanum complex 13, is sufficiently soluble for its infrared spectrum to be measured, thus allowing a comparison to be made between solid-state and solution structures. The carbonyl and perchlorate bands occur at very similar frequencies in  $\text{CDCl}_3$  and in spectra recorded as Nujol mulls, indicating that the solid-state structure is retained in chloroform solution. The <sup>31</sup>P NMR spectrum in  $\text{CDCl}_3$  shows two peaks at  $\delta$  35.0 and 36.4, the latter agreeing well with the observed shift in nitromethane. The two signals could arise from the presence of ionisation isomers  $[\text{La}(\text{ClO}_4)_2(\text{pdppo})_4(\text{OH}_2)][\text{ClO}_4]$  13a and  $[\text{La}(\text{ClO}_4)(\text{pdppo})_4(\text{OH}_2)]_2[\text{ClO}_4]_2$  13b. In the more ionising solvent the formation of 13b would be favoured, and the peak at  $\delta$  36.4 is assigned to this isomer.

To establish the presence of free perchlorate ions in solution, attempts were made to measure the <sup>35</sup>Cl NMR spectrum. The spectrum of aqueous  $\text{ClO}_4^-$  is readily obtained as a sharp signal. Similarly triethylamine hydroperchlorate gives a sharp signal in  $\text{CDCl}_3$ . Attempts to detect <sup>35</sup>Cl signals from the lanthanum complex in  $\text{CDCl}_3$  or nitromethane solutions failed. This is presumably due to association of the perchlorate ion with the cation, which causes sufficient distortion from tetrahedral geometry to broaden the <sup>35</sup>Cl signal rendering it unobservable. In view of the large line broadening factor for <sup>35</sup>Cl, the non-observation of the signal is not surprising.<sup>24</sup> Similarly, no observable signals would be expected from coordinated perchlorate, where a much greater reduction in the symmetry of the ion occurs.

Although solution infrared spectra could not be obtained for the other complexes due to low solubility, those of Ce, Pr and Nd were sufficiently soluble to permit <sup>31</sup>P NMR spectra to be obtained on prolonged accumulation. In each case a single resonance only was observed at chemical shifts different from those observed in nitromethane. Thus complex 14 gave a signal at  $\delta$  58.9 compared with 54.1 in nitromethane, whilst 15 gave a signal at  $\delta$  94.6 compared with 78.6 and 16 gave a peak at  $\delta$  86.4 as opposed to 71.7. It thus seems that the solid-state structure is present in solution, at least for the lanthanum complex. For the other complexes it is not possible to deduce whether the solid-state structure is retained in solution. However, the <sup>31</sup>P NMR spectra do indicate structural differences between chloroform and nitromethane solution.

*Complexes of dbpp.*—All the complexes of this ligand were synthesised as intractable oils which proved impossible to crystallise. It was thus much more difficult to purify the compounds and representative elemental analyses were obtained for only some members of each series. The characterising data are given in Table 5.

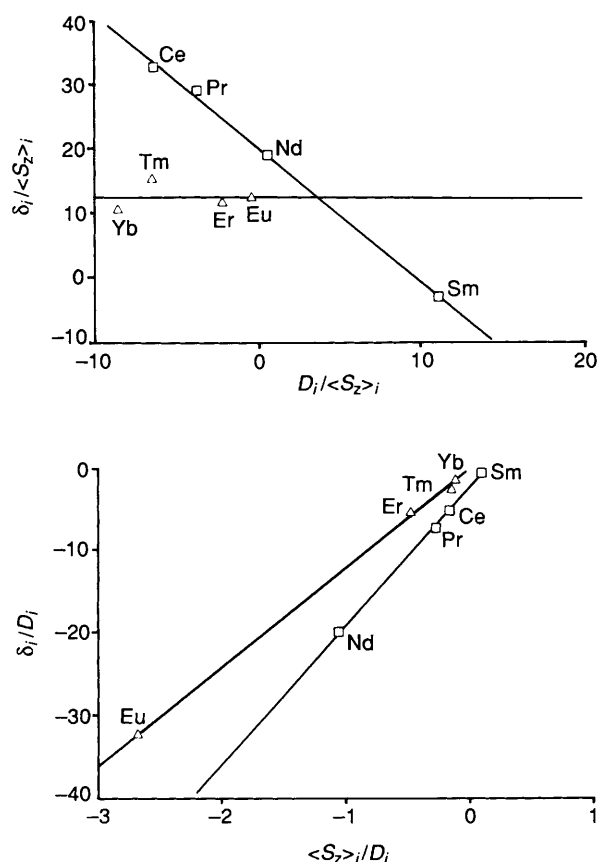


Fig. 5 Plots of the lanthanide-induced shifts for perchlorate complexes of dbpp

**Nitrates.** The elemental analyses of complexes **27** and **31** indicate that there are no changes in composition across the series and that they have the formula  $[\text{Ln}(\text{NO}_3)_3(\text{dbpp})_4(\text{OH}_2)_2]$ . The infrared spectra also indicate that the complexes are isostructural, all giving essentially identical spectra with a single CO absorption at  $1675 \text{ cm}^{-1}$  (unchanged from its position for dbpp) and two PO stretches at  $1220$  and  $1180 \text{ cm}^{-1}$  (compared with  $1270$  and  $1250 \text{ cm}^{-1}$  for dbpp). From these data it would seem that the ligand is bound by the phosphoryl oxygen atom only, and that the carbonyl group is not chelating to the metal or hydrogen-bonding to the co-ordinated water. The nitrate groups show the typical absorption bands associated with bidentate co-ordination. These data imply that the lanthanide ions are twelve-co-ordinate.

Analysis of the NMR data shows that both plots of  $\delta_i / \langle S_z \rangle_i$  vs.  $D_i / \langle S_z \rangle_i$  and  $\delta_i / D_i$  vs.  $\langle S_z \rangle_i / D_i$  are linear, although there is considerable scatter about the latter plot, with regression coefficients of  $0.94$  and  $0.55$  respectively, implying that the complexes are isostructural in solution. From the limited amount of data available it seems that these complexes are twelve-co-ordinate both in solution and as the isolated complexes.

**Perchlorates.** Elemental analyses were carried out on the complexes of Pr and Er chosen as being representative of the lighter and heavier lanthanides. A change in composition was indicated with the lighter lanthanides having a formula  $[\text{Ln}(\text{ClO}_4)_3(\text{dbpp})_4(\text{OH}_2)_2]$  whilst the heavier elements appear to accommodate three dbpp ligands, giving compositions  $[\text{Ln}(\text{ClO}_4)_3(\text{dbpp})_3(\text{OH}_2)_2]$  consistent with the decrease in ionic radii. Although no regular trend in the infrared spectra is seen, there are differences as shown in Table 5. Thus decreases in  $\nu_{\text{PO}}$  and  $\nu_{\text{CO}}$  are evident for all complexes and indicate either that dbpp is either chelating or hydrogen-bonding to the co-ordinated water molecules. However, the spectra for some of the complexes, of Pr, Sm, Eu, Yb and Lu, show an additional band

at  $1670 \text{ cm}^{-1}$ , indicative of uncomplexed CO. This implies the presence of monodentate dbpp, but there is no obvious pattern to the occurrence of this bonding mode across the series. Analysis of the bands due to the perchlorate groups is again complicated by the presence of the PO absorptions and the overlap of bands due to bonded perchlorate.

The  $^{31}\text{P}$  NMR data give a strong indication of major structural changes for the species in solution, which agree broadly with the compositions of the complexes of the lighter and heavier elements. Thus both plots of  $\delta_i / \langle S_z \rangle_i$  vs.  $D_i / \langle S_z \rangle_i$  and  $\delta_i / D_i$  vs.  $\langle S_z \rangle_i / D_i$  show two distinct lines for La–Sm and Eu–Lu as shown in Fig. 5. These data imply strongly that the changes in co-ordination number which were indicated for the isolated complexes are also reflected in the solution structures.

## Conclusion

The analysis of lanthanide-induced shifts for a series of related complexes seems to give a reliable indication of uniformity, or otherwise, of solution structures. In the case of the nitrate complexes of pdppo, where definitive solid-state information is available, it is evident that the solution structures are different.

## Experimental

The ligands pdppo<sup>25</sup> and dbpp<sup>26</sup> were prepared by literature methods. Complexes were prepared by the same general method, that is by adding an ethanol solution of the metal nitrate or perchlorate to a refluxing solution of an excess of the ligand in ethanol. In the case of the nitrates, the complexes precipitated as solids (pdppo) or oils (dbpp) on cooling. The perchlorates precipitated immediately from solution on mixing. The solid complexes were filtered off, washed with hot ethanol and dried *in vacuo*. The complexes of dbpp were separated by decantation, the remaining oil being triturated with hot ethanol and dried *in vacuo*. The nitrate complexes were obtained in yields of around 70% and the perchlorates quantitatively. All complexes had the characteristic colour of the lanthanide ions.

The  $^{31}\text{P}$  NMR spectra were recorded at  $36.23 \text{ MHz}$  on a JEOL FX90Q spectrometer in  $10 \text{ mm}$  tubes. With non-deuterated solvents, the NMR lock was provided by a capillary tube containing  $\text{D}_2\text{O}$ . Infrared spectra were recorded on a Perkin-Elmer 457 spectrometer as either Nujol mulls or KBr discs for solids or in a  $0.1 \text{ mm}$  path length cell for solution spectra. Spectra of dbpp complexes were obtained as contact films.

**Crystallography.**—*Crystal data.*  $\text{C}_{40}\text{H}_{34}\text{ErN}_3\text{O}_{13}\text{P}_2 \cdot \text{H}_2\text{O}$  **10**,  $M = 1011.94$ , triclinic space group  $P\bar{1}$ ,  $a = 11.274(15)$ ,  $b = 18.662(18)$ ,  $c = 11.65(2) \text{ \AA}$ ,  $\alpha = 109.0(1)$ ,  $\beta = 114.0(1)$ ,  $\gamma = 89.5(1)^\circ$ ,  $U = 2096.9 \text{ \AA}^3$ ,  $Z = 2$ ,  $D_c = 1.602 \text{ g cm}^{-3}$ ,  $\mu = 20.19 \text{ cm}^{-1}$ ,  $F(000) = 993.9$ .

The unit-cell parameters were determined from an oscillation photograph for the rotation axis  $c$ , and from refined positional data of zero- and upper-layer reflections. The crystal dimensions were  $0.28 \times 0.18 \times 0.36 \text{ mm}$ . The intensities of 8812 unique reflections with  $2\theta < 54^\circ$  and  $\pm h, \pm k, \pm l$  were measured on a Stoe STADI-2 Weissenberg diffractometer, with graphite monochromated Mo-K $\alpha$  radiation ( $\lambda = 0.7107 \text{ \AA}$ ) using an  $\omega$ -scan technique. The data were corrected for Lorentz and polarisation effects to yield 6898 reflections with  $I > 3\sigma(I)$ . An absorption correction was applied to the data with maximum and minimum transmission factors  $0.729$  and  $0.584$  respectively.

The structure was solved using the PATT option of SHELXS 86.<sup>27</sup> All subsequent calculations were carried out using the computer program SHELX 76.<sup>28</sup> The hydrogen atoms of the water molecule were located and refined. All other hydrogen atoms were included in calculated positions (C–H  $1.08 \text{ \AA}$ ), with a single fixed thermal parameter. The non-hydrogen atoms were refined with anisotropic thermal parameters.

Final cycles of refinement employed a weighting parameter  $g = 0.00068$  in  $w = 1/[\sigma^2(F) + g(F)^2]$  and gave the final residual indices  $R = \sum(|F_o| - |F_c|)/\sum|F_o| = 0.028$  and  $R' = [\sum w(|F_o| - |F_c|)^2/\sum w|F_o|^2]^{1/2} = 0.031$ . The final Fourier difference map was featureless and an analysis of the weighting scheme over  $|F_o|$  and  $\sin \theta/\lambda$  was satisfactory.

Additional material available from the Cambridge Crystallographic Data Centre comprises H-atom coordinates, thermal parameters and remaining bond lengths and angles.

### Acknowledgements

Thanks are due to the Leicester University Computer centre, who provided support and facilities for the X-ray single-crystal calculations. We also thank ICI Organics (Blackley) for some financial assistance.

### References

- 1 F. Matsumoto, T. Takewchi and A. Ouchi, *Bull. Chem. Soc. Jpn.*, 1981, **62**, 1809.
- 2 W. J. Evans, T. J. Deming, J. M. Olofson and J. W. Ziller, *Inorg. Chem.*, 1989, **28**, 4027.
- 3 D. J. Berg, S. J. Rettig and C. Orvig, *J. Am. Chem. Soc.*, 1991, **113**, 2528.
- 4 A. J. Fry and M. Sala, *J. Am. Chem. Soc.*, 1989, **111**, 3225.
- 5 S. Warren, RSC Autumn Meeting, University of Keele, 1990, Perkin Division, Abstract 607.
- 6 M. Th. Youinov and J. E. Guerschias, *Inorg. Chim. Acta*, 1976, **19**, 257.
- 7 J. C. Martin and M. J. F. Leroy, *J. Chem. Res.*, 1978, (S) **88**, (M) 1113.
- 8 C. M. Mikulski, W. Henry, L. L. Pytlewski and N. Karayanis, *J. Inorg. Nucl. Chem.*, 1978, **40**, 769.
- 9 M. Burgard and B. Ceccaroll, *J. Phys. Chem.*, 1982, **86**, 4817.
- 10 B. Ceccaroll, J. Alsd and M. J. F. Leroy, *Polyhedron*, 1982, **1**, 257.
- 11 J. A. Peters, *J. Magn. Reson.*, 1986, **68**, 240.
- 12 P. Rubini, C. Ben Nasr, L. Rodehuser and J.-J. Delpuech, *Magn. Reson. Chem.*, 1987, **25**, 609.
- 13 R. Babecki, A. W. G. Platt and D. R. Russell, *Inorg. Chim. Acta*, 1990, **171**, 25.
- 14 S. M. Bowen, E. N. Duesler and R. T. Paine, *Inorg. Chim. Acta*, 1982, **61**, 155.
- 15 D. J. McCabe, E. N. Duesler and R. T. Paine, *Inorg. Chem.*, 1985, **24**, 4626.
- 16 D. J. McCabe, E. N. Duesler and R. T. Paine, *Inorg. Chem.*, 1988, **27**, 1220.
- 17 R. D. Rogers, A. N. Rollins and M. M. Benning, *Inorg. Chem.*, 1988, **27**, 3826.
- 18 Y. Kawano and V. K. Lakatos Osorio, *J. Inorg. Nucl. Chem.*, 1977, **39**, 701.
- 19 D. G. Hendricker and R. J. Foster, *J. Inorg. Nucl. Chem.*, 1972, **34**, 1949.
- 20 K. Nakamoto, *Infrared and Raman Spectra of Inorganic and Coordination Compounds*, Wiley, New York, 1986.
- 21 R. M. Golding and M. B. Halton, *Aust. J. Chem.*, 1972, **25**, 2577.
- 22 R. M. Golding and Pyykko, *Mol. Phys.*, 1972, **26**, 1389.
- 23 W. Geary, *Coord. Chem. Rev.*, 1971, **7**, 81.
- 24 R. K. Harris, *Nuclear Magnetic Resonance Spectroscopy*, Pitman, London, 1983, p. 232.
- 25 A. D. Buss, W. B. Cruse, O. Kennard and S. Warren, *J. Chem. Soc., Perkin Trans. 1*, 1984, 243.
- 26 M. G. Imaev, A. M. Shakirova, E. P. Sirmanova and E. K. Kas'janova, *Zh. Obshch. Khim.*, 1964, **34**, 3950.
- 27 G. M. Sheldrick, SHELXS 86, Program for crystal structure solution, University of Göttingen, 1986.
- 28 G. M. Sheldrick, SHELXS 76, Program for crystal structure determination, University of Cambridge, 1976.

Received 15th May 1991; Paper 1/02295D